Adaptive Mesh Refinement Procedure for Shear Localization Problems

Hyun-Gyu Kim*
Department of Mechanical Engineering, Seoul National University of Technology, 172 Gongneung-2dong, Nowon-gu, Seoul 139-743, Korea
Seyoung Im
Department of Mechanical Engineering, Korea Advanced Institute of Science and Technology, Science Town, Taejon 305-701, Korea

The present work is concerned with the development of a procedure for adaptive computations of shear localization problems. The maximum jump of equivalent strain rates across element boundaries is proposed as a simple error indicator based on interpolation errors, and successfully implemented in the adaptive mesh refinement scheme. The time step is controlled by using a parameter related to the Lipschitz constant, and state variables in target elements for refinements are transferred by L_2-projection. Consistent tangent moduli with a proper updating scheme for state variables are used to improve the numerical stability in the formation of shear bands. It is observed that the present adaptive mesh refinement procedure shows an excellent performance in the simulation of shear localization problems.

Key Words: Finite Elements, Error Indicator, Mesh Refinement, Adaptivity, Shear Localization

1. Introduction

When shear localization problems are simulated numerically, one encounters a difficulty of multi-scale phenomena accompanied by a strong concentration of the plastic strain in a narrow band. A very fine mesh or a special technique is required to treat extremely large strain gradients across a shear band. Adaptive methods may be a natural choice for overcoming this difficulty in that the structure of a shear band is generally unknown before computations.

Since the full discretization into a fine mesh requires a huge amount of computation time for the shear localization problems, adaptive mesh refinement techniques have been employed to refine the mesh where needed. In performing the adaptive mesh refinement, a key issue is to determine a posteriori error in computations, which indicates regions to be refined for improving the accuracy in subsequent calculations. Many error indicators based on residual methods (Babuska and Rheinboldt, 1978), projection methods (Zienkiewicz and Zhu, 1991) and interpolation error methods (Demkowicz et al., 1985) have been developed for linear problems. These error indicators have been successfully used with equivalency among them in linear elasticity problems (Zhu, 1997). Unfortunately, the error indicators developed in linear problems may give us information far from true errors in nonlinear problems. Particularly, error indicators based on the ellipticity may not apply for localization problems, because the governing equations almost lose the ellipticity in numerical simulations. Belytschko and Tabbara (1993) showed that the error indicators based on the re-

* Corresponding Author,
E-mail : khg@snut.ac.kr
TEL : +82-2-970-6309; **FAX** : +82-2-949-1458
Department of Mechanical Engineering, Seoul National University of Technology, 172 Gongneung-2dong, Nowon-gu, Seoul 139-743, Korea. (Manuscript **Received** August 7, 2006; **Revised** September 8, 2006)

sidual and the stress projection methods do not present proper errors in localization problems. Ortiz and Quigley (1991) proposed the error indicator of the velocity variation for the analysis of shear localization. Batra and Ko (1992) used the rate of deformation and Khoei and Lewis (2002) the maximum gradient of displacements. A great deal of effort is still required to develop an efficient error indicator for shear localization problems.

In our study, we propose a simple and reliable error indicator based on interpolation errors. Since interpolation error methods do not rely on the type of governing equations, it may be suited to develop a proper error indicator for localization problems. The proposed error indicator is the maximum jump of equivalent strain rates across element boundaries, and we use this error indicator as a basis for adaptively refining the mesh. The state variables in enriched elements are transferred by L_2-projection, and those in the other elements are directly inherited from the parent mesh, which reduces the numerical diffusion. The time step, which is an important parameter for the numerical stability, is controlled by employing the concept of the Lipschitz constant. The state variables are updated by using iterative backward Euler methods with initial values from forward gradient methods, and consistent tangent moduli are implemented in the coupled equations.

2. Governing Equations

The governing equations with the inertia term neglected are written as

$$\frac{\partial \boldsymbol{\sigma}}{\partial \boldsymbol{x}}=0 \tag{1}$$

$$\rho c\frac{d\theta}{dt}=\frac{\partial}{\partial \boldsymbol{x}}\left(x\frac{\partial \theta}{\partial \boldsymbol{x}}\right)+\kappa\boldsymbol{\sigma}:\boldsymbol{D}^{p} \tag{2}$$

where $\boldsymbol{\sigma}$ is the stress, θ is the temperature, $\boldsymbol{D}^{p}$ is the plastic rate of deformation, ρ is the density, c is the specific heat, k is the thermal conductivity, and k is the fraction of the plastic work converted into heat energy. We use the constitutive model described by the additive decomposition of the strain tensor into elastic and plastic parts:

$$\dot{\boldsymbol{\sigma}}^{J}=\boldsymbol{L}:(\boldsymbol{D}-\boldsymbol{D}^{p}) \tag{3}$$

In the above equation, $\dot{\boldsymbol{\sigma}}^{J}$ is the Jaumann stress rate and the elastic modulus $\boldsymbol{L}$ defined as

$$\boldsymbol{L}=2\mu\boldsymbol{II}+\left(\Im-\frac{2}{3}\mu\right)\boldsymbol{I}\otimes\boldsymbol{I} \tag{4}$$

where μ and $\Im$ are the shear and the bulk moduli, respectively, and $\boldsymbol{II}$ and $\boldsymbol{I}$ denote the unit fourth and second order tensors, respectively. The plastic rate of deformations is defined as follows:

$$\boldsymbol{D}^{p}=\sqrt{\frac{3}{2}}\dot{\bar{\varepsilon}}^{p}\boldsymbol{N} \tag{5}$$

$$\boldsymbol{N}=\sqrt{\frac{3}{2}}\frac{\boldsymbol{\sigma}'}{\bar{\sigma}} \tag{6}$$

$$\dot{\bar{\varepsilon}}^{p}=f(\bar{\sigma},\ \bar{\varepsilon}^{p},\ \theta) \tag{7}$$

where $\bar{\sigma}$, $\boldsymbol{\sigma}'$ and $\bar{\varepsilon}$ are the effective stress, the deviatoric stress and the equivalent plastic strain, respectively.

3. Computational Algorithms

The coupling of displacement and temperature fields appears in numerical computations for thermo-viscoplastic material models. Conventionally, the coupled equations (1) and (2) are solved by the staggered algorithm in which the mechanical field variables are fixed during the calculation of thermal fields and the converse is taken for the calculation of mechanical fields. This solution technique may produce numerical instabilities in a highly nonlinear problem. Hence, we simultaneously solve the coupled equations with consistent tangent moduli and with a proper updating scheme for state variables.

Simple Euler forward procedures have a tendency to be easily unstable unless the step size is very small. One can improve the numerical stability by taking semi-implicit types of time integrations like the forward gradient methods (Peirce et al., 1984). Although the forward gradient schemes are advantageous in that the consistent tangent moduli and the implementation are straightforward, numerical instabilities may be encountered for a highly nonlinear problem. In general, the iterative backward Euler methods with a proper initial guess (Lush et al., 1989) have more stable

behaviors than the methods mentioned previously. We choose the iterative backward Euler methods with the initial guess obtained from the forward gradient methods for updating state variables, and develop consistent tangent moduli in coupled thermo-mechanical problems. It should be noted that the consistency between the integration scheme and the tangent moduli is important to obtain a good convergence rate of the Newton-Raphson iterations.

4. Adaptive Mesh Refinement

4.1 Error Indicator

The objective of this section is to develop a proper error indicator for adaptive meshing in localization problems. Considering the interpolation error methods do not rely on the ellipticity of the governing equations, we use the errors associated with the interpolations. It should be noted that the error indicators based on the ellipticity break down in localization problems, because the governing equations lose or nearly lose the ellipticity in the development of shear bands. The error for the finite element solution $\Delta \boldsymbol{u}^h$ of $\Delta \boldsymbol{u}$ has the following bound associated with the interpolation $\prod \Delta \boldsymbol{u}$ of $\Delta \boldsymbol{u}$.

$$\|\Delta \boldsymbol{u}^h - \Delta \boldsymbol{u}\| \leq C \|\prod \boldsymbol{u} - \Delta \boldsymbol{u}\| \tag{8}$$

where C is a positive constant, and $\|\cdot\|$ is a Sobolev norm. Note that $\Delta \mathbf{u}^h$ is the displacement increment in a time step. Let "k" indicate the order of interpolations or the degree of complete polynomials in interpolation functions. We assume that the solution $\Delta \boldsymbol{u}$ is smooth in the sense that $\Delta \boldsymbol{u} \subset H^{k+1}$, where H^{k+1} denotes the Sobolev function space of order $k+1$. Then the error found for $\Delta \boldsymbol{u}$ in the domain Ω is given as, see Ciarlet (1978),

$$\|\prod \Delta u - \Delta \boldsymbol{u}\|_m \leq c h^{k+1-m} |\Delta \boldsymbol{u}|_{k+1},\ 0 \leq m \leq k \tag{9}$$

where c is a positive constant, h represents the maximum element size, and $|\cdot|_{k+1}$ is the semi-norm associated with the norm $|\cdot|_{k+1}$ of H^{k+1}. This result is related to the ability of resolving the solutions by interpolations of order k. The bounds on the interpolation error in the Sobolev space may be immediately available as an error indicator for finite element approximations to solutions of localization problems. In our analyses, we use only linear elements ($k=1$), and with the choice of $m=1$ then be obtained as

$$\|\prod \Delta \boldsymbol{u} - \Delta \boldsymbol{u}\|_1 \leq c h |\Delta \boldsymbol{u}|_2 \tag{10}$$

We are concerned with interpolation errors in elements for finding mesh sizes in subsequent computations to improve the accuracy of solutions with a better mesh. Let the problem domain be discretized into finite element space Ω_I, $I=1,\cdots,M$. The problem of finding an estimate for the error $\|\Delta \mathbf{u}^h - \Delta \mathbf{u}\|_1$ is reduced to the problems of evaluating quantities such as $\|\prod \Delta \mathbf{u} - \Delta \mathbf{u}\|_{1,\Omega_I}$. As a consequence, the following interpolation errors of elements I are defined by

$$e_{\Omega_I} = h_I \left(\int_{\Omega_I} \Delta u_{i,jk} \Delta u_{i,jk} d\Omega \right)^{1/2} \tag{11}$$

where a comma stands for partial differentiation, and repeated indices imply summation. The interpolation error in the global domain is furnished by $e_\Omega = \sum_{I=1}^{M} e_{\Omega_I}$. Since the strain increments have lower order than the displacement increments in finite elements, the error estimate (11) may not be directly evaluated in the finite element domains. Particularly, a special technique is required to define errors in finite elements. For instance, Demkowicz et al. (1985) used an extract formula for accurate estimates of higher derivatives. For the sake of simplicity, we use the equivalent strain increment defined by $\Delta \bar{\varepsilon} = \sqrt{2 \Delta \varepsilon_{ij} \Delta \varepsilon_{ij}/3}$ instead of the gradients of displacement increments in Eq. (11). The equivalent strain used here approaches to the equivalent plastic strain as the plastic strain is dominant in deformations. In shear localization problems, the integral term in Eq. (11) is then approximated by

$$\int_{\Omega_I} \Delta u_{i,jk} \Delta u_{i,jk} d\Omega \approx \int_{\Omega_I} \Delta \bar{\varepsilon}_{,k} \Delta \bar{\varepsilon}_{,k} d\Omega \tag{12}$$

Applying the Friedrichs inequality to Eq. (12) yields

$$\begin{aligned} \int_{\Omega_I} \Delta \bar{\varepsilon}_{,k} \Delta \bar{\varepsilon}_{,k} d\Omega &\leq c_1 \int_{\Omega_I} \Delta \bar{\varepsilon}_{,kl} \Delta \bar{\varepsilon}_{,kl} dx \\ &+ c_2 \int_{\Gamma_I} \Delta \bar{\varepsilon}_{,k} \Delta \bar{\varepsilon}_{,k} d\Gamma \end{aligned} \tag{13}$$

where c_1 and c_2 are positive constants, and Γ_I are the boundaries of elements I as shown in Fig. 1. In our study, $\Delta\bar{\varepsilon}$ is replaced by $\Delta\bar{\varepsilon}^h$ to estimate interpolation errors of elements, which will give better results as the mesh size decreases. The first term in the right-hand side of Eq. (13) vanishes, because the third order derivatives of $\Delta\bar{\varepsilon}^h$ become zero in linear elements. Hence, interpolation errors of elements I are rewritten as

$$e^h_{\Omega_I} = h_I \left(\int_{\Gamma_I} \Delta\bar{\varepsilon}^h_{,k} \Delta\bar{\varepsilon}^h_{,k} d\Omega \right)^{1/2} \tag{14}$$

Since there is a jump in the derivatives of $\Delta\bar{\varepsilon}^h$ on an interelement boundary, the derivatives of the equivalent strain increments in the normal directions on element boundaries will be undefined. Now, the jump of the equivalent strain increments across element boundaries may be a measure of interpolation errors in that the derivatives in Eq. (14) are directly related to the difference between the equivalent strain increments of adjacent elements. As a result, interpolation errors of linear elements can be evaluated by a simple indicator such as

$$e^h_{\Omega_I} = h_I \max_I [\dot{\bar{\varepsilon}}^h]_{\Gamma_I} \tag{15}$$

where $\dot{\bar{\varepsilon}}$ is the equivalent strain rate, $[\dot{\bar{\varepsilon}}^h] = |\dot{\bar{\varepsilon}}^{h+}\mathbf{n}^+ + \Delta\dot{\bar{\varepsilon}}^{h-}\mathbf{n}^-|$, and $\mathbf{n}^+$ and $\mathbf{n}^-$ are the unit normal vectors indicated in Fig. 1. If the jump of strain rates between adjacent elements is large, the interpolation error (15) is also large due to high gradients of the strain rates. The present error indicator implies that the mesh in high gradients of the equivalent strain rate should be refined, which is matched with the general concept of adaptive mesh refinement strategies. The equivalent strain rate itself was used for the error indicator, but its gradients appear to be more proper in that no adaptive refinement is needed for a region of high strain rate if the region has a uniform strain rate. Furthermore, the present error indicator is relatively inexpensive and convenient to use in comparison to the procedures using projection types of error indicators.

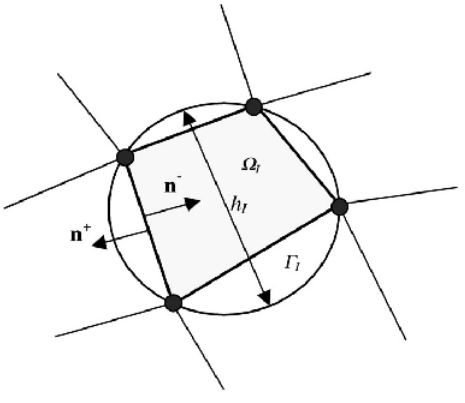

Fig. 1 Unit normal vectors $\mathbf{n}^+$ and $\mathbf{n}^-$ on boundaries Γ_I of the finite element domains Ω_I with mesh sizes h_I

4.2 Mesh refinement strategy

It has been generally known that an optimal mesh may be constructed when the error of each element has the same value in all elements (Zhu, 1997). In our analyses, we refine some elements in case the error obtained from Eq. (15) has a larger value than a permissible error. The target elements for refinements are selected by

$$e^h_{\Omega_I} \geq \eta \frac{e^h_\Omega}{M} \tag{16}$$

where η is a value specified by user, and M is the total number of elements. The final goal of the mesh refinement is to find an optimal mesh that provides equi-distributed errors over elements. We use the linear quadrilateral and the triangular elements in our finite element calculations. As

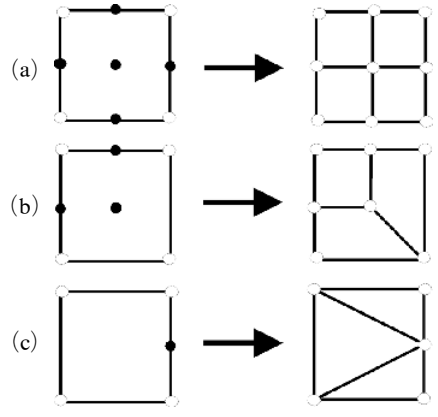

Fig. 2 Refinements for a target element and neighboring elements : (a) the target element is divided into four elements, and the neighboring elements are processed as shown in (b) and (c)

shown in Fig. 2, the target elements for refinement are divided by four successor elements, and the neighboring elements are also divided into three quadrilateral elements or three triangular elements because they cannot be connected solely by four-noded quadrilaterals. Since linear triangular elements inside shear bands yield locking due to the incompressibility of plastic deformations (Belytschko et al., 1994), we use the triangular elements only in an elastic unloading region or in a far field from the band center.

4.3 State variable transfer and time step control

For history dependent problems, the solution procedures cannot be re-computed from scratch, as the mesh is refined through an appropriate error indicator. Therefore, one of important points in adaptive mesh refinement procedures is the transfer of state variables such as stresses, strains and others. Projection types of transfer operators were explained by Peric et al.(1996), and patch recovery types were presented by Zienkiewicz and Zhu (1992). In general, projection procedures have been reported to smear localization modes into outer regions, and patch recovery has a far more negative effect. One suggestion for limiting the diffusion of localized deformations into the non-localized region is the selective projection procedure. In this method, the state variables in the target elements for refinements are transferred by L_2-projection wherein all elements are involved. On the other hand, the state variables in elements with no refinement are directly transferred from the parent elements. This selective projection procedure is helpful for preserving the limit diffusion of localized deformations.

The stiff behaviors of the governing equations restrict the time step size near the critical time for the severe localization. In the ordinary differential equations, the time step in an implicit iteration is confined by the magnitude of the Lipschitz constant (Aiken, 1985). Numerical solutions of a problem with a large Lipschitz constant may diverge rapidly in a relative sense. With the same concept, a parameter J related to the Lipschitz constant is defined by

$$J \equiv \max_x \left| \frac{\Delta \dot{\bar{\varepsilon}}}{\Delta \bar{\varepsilon}} \right| \tag{17}$$

A sufficient condition for convergence in the backward Euler method for the ordinary differential equations is $\Delta t J < 1$ (Aiken, 1985). Hence, the following scheme to restrict the step size in computations for localization problems is proposed as

$$\begin{cases} \Delta t = \dfrac{J_{ref}}{J} \Delta t_{ref}, & \text{if } J > J_{ref} \\ \Delta t = \Delta t_{ref}, & \text{otherwise} \end{cases} \tag{18}$$

where Δt_{ref} and J_{ref} are the reference time step and parameter related to the Lipschitz constant. A large value of the parameter J due to a rapid change of the equivalent strain rate leads to a small time step.

5. Numerical Results

In this section, a number of representative numerical experiments for shear localizations in the plane strain are presented by using the adaptive mesh refinement techniques described in the previous sections. We consider the flow rule used by Lemonds and Needleman (1986).

$$\dot{\bar{\varepsilon}}^p = \dot{\bar{\varepsilon}}_0^p \left[\frac{\bar{\sigma}}{\bar{\sigma}_0 (1 - \alpha\theta)} \right]^{\frac{1}{m}} \left(1 + \frac{\bar{\varepsilon}^p}{\bar{\varepsilon}_0^p} \right)^{-\frac{N}{m}} \tag{19}$$

The material properties used in this study are listed in Table 1, and the strain hardening exponent N is taken to be zero on the same lines of numerical experiments for the simple shear problems by Kim and Im (1998). The two-fold symmetric condition is imposed on $x_1=0$ and $x_2=0$ lines for the model shown in Fig. 3, and the velocity V_0 is

Table 1 Material properties

Properties	Symbols	Values
Density	ρ	7833.0 kg/m^3
Specific heat	c	465.0 J/kgK
Thermal conductivity	k	54.0 W/mK
Dissipation factor	κ	1.0
Shear modulus	μ	2.0×10^{11} N/m^2
Reference shear stress	$\bar{\sigma}_0$	1.25×10^{9} N/m^2
Strain rate sensitivity	m	0.01
Reference strain rate	$\dot{\bar{\varepsilon}}_0$	$1.0\times10^{-3}s^{-1}$
Softening coefficient	α	$1.6\times10^{-3}K^{-1}$

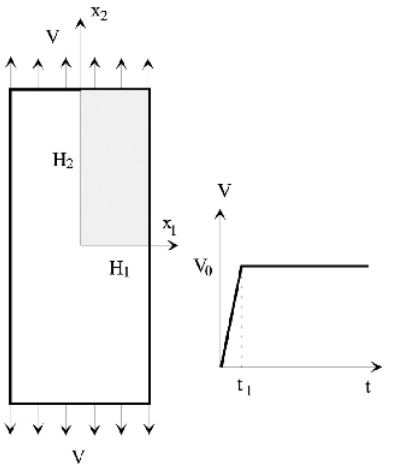

Fig. 3 Two-dimensional model under the velocity boundary condition

3 m/s after $t_1=1\times10^{-6}$ sec. The symmetric model width H_1 and height H_2 are 1.5 mm×3.0 mm. We initially discritize the model into 20×10 quadrilateral elements. We impose the initial temperature perturbation such as

$$\theta(x_1,x_2)=\begin{cases}\theta_\epsilon\left(1-\dfrac{x_1^2+x_2^2}{H_1^2}\right)^9 e^{-5\left(\frac{x_1^2+x_2^2}{H_1^2}\right)}, & \text{if } x_1^2+x_2^2<H_1^2\\ 0, & \text{otherwise}\end{cases} \quad (20)$$

In our calculations, we take θ_ϵ to 2℃. The lumped mass is used for the heat capacity term in order to preserve the stability, and one point integration for linear elements with a weak hour-glass control is used in calculations.

We take the value η in Eq. (16) to be 1.2, and the permissible maximum error for refinements to be 2.0. A small value of η tends to broaden the region of refinements, and a large permissible error reduces the total number of refinements. Firstly, we examine the effect of mesh refinements to the localization behavior by restricting the maximum number of refinements. The critical time of the stress collapse shows similar points (see Fig. 4) for different meshes. It does mean that the mesh refinements do not affect the critical time of a severe localization. The average stress and the maximum equivalent plastic strain rate with the constraint of the maximum number of refinements are compared for different meshes in Figs. 4 and

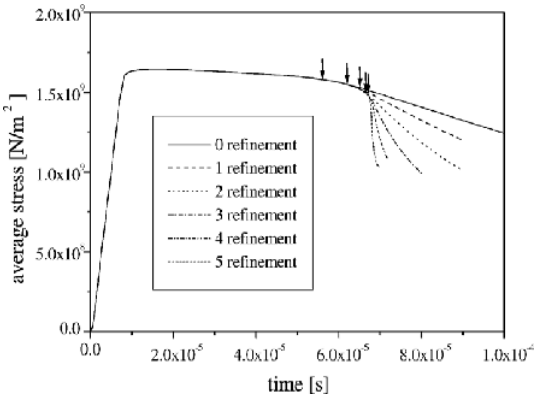

Fig. 4 Average stresses for different meshes. Mark ↓ indicates the inception points of mesh refinements

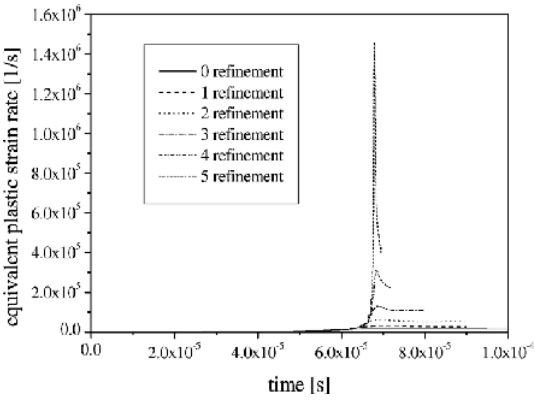

Fig. 5 Maximum equivalent plastic strain rates for different meshes

5. The inception points of mesh refinements are marked in Fig. 4. On the contrary to the critical time of the stress collapse, the evolutions of the average stress and the maximum equivalent plastic strain rate are shown to be significantly different depending upon the level of refinements. More refined is the mesh, the higher is the stress drop rate, and the maximum equivalent plastic strain rate tends to overshoot more severely during the stress collapse. Consequently, coarse meshes cannot represent well the process of the stress collapse.

With five steps of mesh refinements, the deformed meshes just before refinements are shown in Fig. 6. Since the errors obtained by the indicator (15) decrease after the refinement by divid-

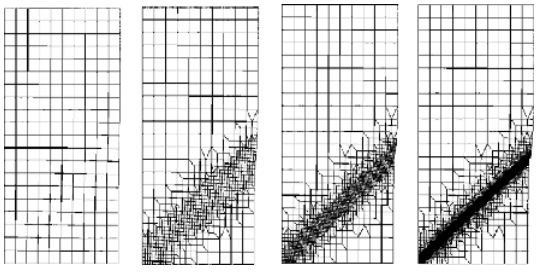

Fig. 6 Deformed meshes: (a) $t=5.6\times10^{-5}s$, (b) $t=6.53\times10^{-5}s$, (c) $t=6.67\times10^{-5}s$, (d) $t=6.9\times10^{-5}s$

ing the target elements into the successor elements, a number of time steps in computations are taken to meet the condition (16) for the next step of mesh refinement as indicated in Fig. 4. In these numerical examples, the time step is successfully controlled by the parameter J related to the Lipschitz constant. The time step is considerably decreased as the strain rates shoot up and down during the stress collapse. In numerical experiments with a very fine mesh, the excessive distortion of elements inside shear bands prevents computations from proceeding to the next steps in the formation of shear bands accompanied with a strong drop of the stress. The temperature and the equivalent plastic strain rate are shown in Figs. 7 and 8, in which the temperature at the final configuration is more spread than the equivalent plastic strain rate. It is apparent from these figures that the shear band defined from the equivalent plastic strain rate is abruptly narrowed during the stress collapse. Consequently, a very fine mesh is required to represent such a narrow band after the critical time. In the present adaptive computations, the oscillatory change of the plastic strain rates just after the mesh refinement is observed, which may be originated from errors in the state variable transfer. However, the oscillatory behavior is decayed out in several time steps after the mesh refinement.

6. Conclusions

A new adaptive mesh refinement procedure is proposed for simulating strain localization prob-

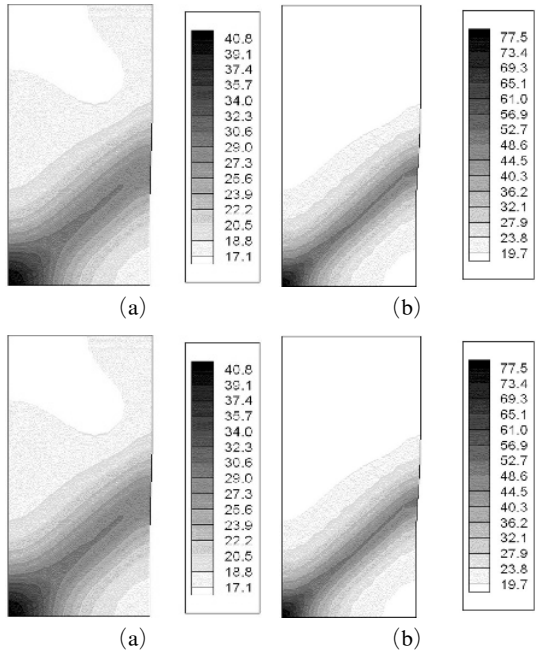

Fig. 7 Temperature: (a) $t=5.6\times10^{-5}s$, (b) $t=6.53\times10^{-5}s$, (c) $t=6.67\times10^{-5}s$, (d) $t=6.9\times10^{-5}s$

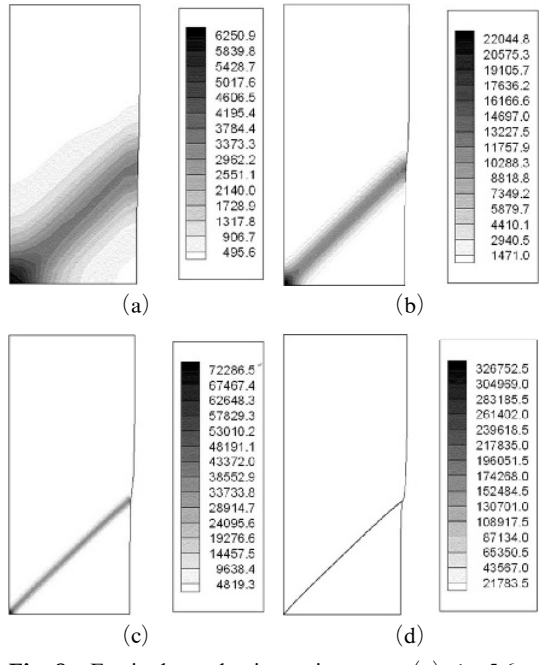

Fig. 8 Equivalent plastic strain rates: (a) $t=5.6\times10^{-5}s$, (b) $t=6.53\times10^{-5}s$, (c) $t=6.67\times10^{-5}s$, (d) $t=6.9\times10^{-5}s$

lems by using the maximum jump of the equiva-

lent strain rates across element boundaries. The proposed error indicator based on interpolation errors is simple and reliable, and successfully implemented in adaptive computations for localization problems. Since interpolation errors do not rely on the ellipticity of the governing equations, the proposed error indicator is suitable for localization problems. In the proposed procedure for adaptive computations, an adaptive time step control associated with the Lipschitz constant is developed. Furthermore, a proper transfer of state variables is implemented, and the consistent tangent moduli with a proper updating scheme for state variables are formulated to improve the numerical stability in the formation of shear bands. The numerical examples show that the present adaptive mesh refinement procedure is very useful enough to detect regions with large gradients of the strain rate.

References

Aiken, R. C., 1985, Stiff Computation, Oxford University Express.

Babuska, I. and Rheinboldt, W. C., 1978, "Error Estimates for Adaptive Finite Element Computations," *SIAM Journal of Numerical Analysis*, Vol. 15, pp. 736～754.

Batra, R. C. and Ko, K. I., 1992, An Adaptive Mesh Refinement Technique for the Analysis of Shear Bands in Plane Strain Compression of a Thermoviscoplastic Solid," *Computational Mechanics*, Vol. 10, pp. 369～379.

Belytschko, T. and Tabbara, M., 1993, "H-adaptive Finite Element Methods for Dynamic Problems, with Emphasis on Localization," *International Journal for Numerical Methods in Engineering*, Vol. 36, pp. 4245～4265.

Belytschko, T., Chiang, H. Y. and Plaskacz, E., 1994, "High Resolution Two-dimensional Shear Band Computations: Imperfections and Mesh Dependence," *Computer Methods in Applied Mechanics and Engineering*, Vol. 119, pp. 1～15.

Ciarlet, P. G., 1978, The Finite Element Method for Elliptic Problems, North-Holland.

Demkowicz, L., Devloo, P. and Oden, J. T., 1985, "On an H-type Mesh-refinement Strategy Based on Minimization of Interpolation Errors," *Computer Methods in Applied Mechanics and Engineering*, Vol. 53, pp. 67～89.

Khoei, A. R. and Lewis, R. W., 2002, "H-adaptive Finite Element Analysis for Localization Phenomena with Reference to Metal Powder Forming," *Finite Elements in Analysis and Design*, Vol. 38, pp. 503～519.

Kim, H.-G. and Im, S., 1999, "Approximate Analysis for Shear Band in a Thermoviscoplastic Material," *ASME Journal of Applied Mechanics*, Vol. 66, pp. 687～694.

Lemonds, J. and Needleman, A., 1986, "Finite Element Analyses of Shear Localization in Rate and Temperature Dependent Solids," *Mechanics of Materials*, Vol. 5, pp. 339～361.

Lush, A. M., Weber, G. and Anand, L., 1989, "An Implicit Time-integration Procedure for a Set of Internal Variable Constitutive Equations for Isotropic Elasto-viscoplasticity," *International Journal of Plasticity*, Vol. 5, pp. 521～549.

Ortiz, M. and Quigley, J. J., 1991, "Adaptive Mesh Refinement in Strain Localization Problems," *Computer Methods in Applied Mechanics and Engineering*, Vol. 90, pp. 781～804.

Peirce, D., Shih, C. F. and Needleman, A., 1984, "A Tangent Modulus Method for Rate Dependent Solids," *Computers & Structures*, Vol. 18, pp. 875～887.

Peric, D., Hochard, C., Dutko, M. and Owen, D. R. J., 1996, "Transfer Operators for Evolving Meshes in Small Strain Elasto-plasticity," *Computer Methods in Applied Mechanics and Engineering*, Vol. 137, pp. 331～344.

Zhu, J. Z., 1997, "A Posteriori Error Estimation — The Relation Between Different Procedures," *Computer Methods in Applied Mechanics and Engineering*, Vol. 150, pp. 411～422.

Zienkiewicz, O. C. and Zhu, J. Z., 1991, "Adaptivity and Mesh Generation," *International Journal for Numerical Methods in Engineering*, Vol. 32, pp. 783～810.

Zienkiewicz, O. C. and Zhu, J. Z., 1992, "The Super-convergent Patch Recovery and a Posteriori Error-estimates, Part I: The Recovery Technique," *International Journal for Numerical Methods in Engineering*, Vol. 33, pp. 1331～1364.